Songklanakarin J. Sci. Technol.
40 (3), 602-608, May - Jun. 2018

http://www.sjst.psu.ac.th

Original Article

A drowsiness detection method based on displacement and gradient vectors

Sorn Sooksatra[1*], Toshiaki Kondo[1], Pished Bunnun[2], and Astuo Yoshitaka[3]

[1] *School of Information and Communication Technology, Sirindhorn International Institute of Technology, Thammasat University, Khlong Luang, Pathum Thani, 12120 Thailand*

[2] *National Electronic and Computer Technology Center, National Science and Technology Development Agency, Khlong Luang, Pathum Thani, 12120 Thailand*

[3] *School of Information Sciences, Japan Advanced Institute of Science and Technology, Ishikawa, 923-1292 Japan*

Received: 11 April 2016; Revised: 26 September 2016; Accepted: 2 March 2017

Abstract

This paper presents a drowsiness detection method for drivers based on visual features in a video sequence. Image intensities are traditionally visual features. However, it is known that they are directly influenced by lighting conditions. We propose a human eye detection method using the normalized cross-correlation between displacement vectors and gradient vectors. Gradient vectors are dependent on lighting conditions but the normalization step makes them independent of illuminations. In this way, the proposed method can detect human eyes regardless of various lighting conditions. We have also found that normalized cross-correlation can be useful, not only for detecting eyes, but also for recognizing open and closed eye states. To overcome poor lighting conditions, we used infrared auxiliary illumination in order to make the proposed method work every moment. The computation speed of the proposed method is fast enough to perform at video rates.

Keywords: drowsiness detection, gradient vectors, displacement vectors, infrared LEDs, face detection

1. Introduction

Drowsiness is a primary safety concern for drivers because it can directly cause traffic collisions. It is difficult for sleepy drivers to pay full attention to the road and its surroundings including traffic lights, road signs, and other vehicles. Recently, the National Highway Traffic Safety Administration (NHTSA) estimates 56,000 road crashes by sleepy drivers annually in the U.S.A. resulting in 40,000 injuries and 1,550 fatalities (Fazli & Esfehan, 2012). It is evident that drowsiness plays a major role in car collisions. Therefore, it is desired to have an automated method to detect driver drowsiness as one of the functions of an advanced driver assistance system (ADAS).

In fact, a drowsiness detection system (DDS) is an important part of an ADAS. A DDS is used to detect and alert drivers when they are sleepy. The techniques for a DDS can be divided into three types: vehicle-based (Ingre *et al.,* 2006; Liu *et al.,* 2009; Salvucci & Liu, 2002); non-visual feature-based (Akin *et al.,* 2008; Healey & Picard, 2005; Kawakita *et al.,* 2010; Kokonozi *et al.,* 2008); and visual feature-based. Vehicle-based techniques use the pattern of driving, such as the movement of the steering wheel and the driving trajectory. However, the pattern depends on the variations of vehicle types and drivers. Second, non-visual feature-based approaches employ special devices to measure the biological signals of the driver. These devices may include an electro-encephalogram, electrocardiogram, electro-oculogram, or

*Corresponding author
Email address: ohm.sorn@gmail.com; tkondo@siit.tu.ac.th

photoplethysmography. The devices are intrusive to the drivers and may not be suitable for daily driving. Third, visual feature-based approaches make use of image data of the driver's face to detect drowsiness. Driver drowsiness is highly associated with the driver's behaviour, such as, yawning, gazing, nodding, and eye closure. The visual feature-based approach may be the most suitable for a DDS because it is not intrusive to drivers and is independent of the variations of vehicle types and drivers. In addition, its equipment is cheaper and easier to install than the other two approaches.

In this paper, we are concerned with the detection of eye closure because it is one of the most important symptoms of drowsiness that appears in the eye (Sigari *et al.,* 2013). This technique is used to measure the percentage of eye closure to recognize the state of the eyes, either open or closed. Typically, people have a blinking rate of 300 ms per blink, and the closed eye duration is 10 ms on average (Anderson *et al.,* 2013). Based on Wilkinson *et al.* (2013), drowsy people have a blinking rate of less than 200 ms per blink and the closed eye duration is more than 500 ms. Therefore, eye-state recognition is related to drowsiness.

In our experiments, lighting situations can be divided into three situations, bright, dim, and dark. Bright and dim situations can be captured by a normal camera (Figures 1a, b) while dark situations can not be seen as illustrated in Figure 1c. To solve this problem, infrared (IR) LEDs are used to illuminate a face in a dark situation, based on our earlier research work (Sooksatra *et al.,* 2015). Since IR LEDs consume little power, they can be used during the day or night without turning them off (Figures 1d-f). IR LEDs also help to increase the visibility of the face in a dim situation (Figure 1e). Therefore, three situations can be illuminated by IR LEDs to improve an eye-state recognition performance, especially in dim and dark situations.

Figure 1. Faces captured without Infrared (IR) illumination in (a) bright, (b) dim, and (c) dark situations, and those with IR illumination in (d) bright, (e) dim, and (f) dark situations.

2. Related work

Many studies have reported on DDSs in terms of eye-state recognition. Edge detection was used to detect the upper and lower eyelids (Fazli & Esfehan, 2012). The gap between them was measured as a percentage of eye closure. Eye states can be recognized by looking at the intensity projection or horizontal projection (Zhang & Zhang, 2006). By using a template of open and closed eye images, zero-mean normalized cross-correlation (ZNCC), as a template matching method, was used by Veeraraghavan and Papanikolopoulos (2001) to find the best match between two templates. By combining these three techniques, better eye state recognition performance was achieved than the one by Yutian *et al.* (2009). They also showed that template matching gave the best performance. However, their methods used grayscale images as an input. Thus, they were subject to lighting conditions. To reduce the effect of lighting conditions, an image enhancement step is added in the DDS by normalizing images with the top-hat filter utilized by Garcia *et al.* (2012). For drivers with eye glasses, Chang *et al.* (2013) shows that correct recognition is lower because eyeglasses may be wrongly considered as eyebrows. For this, they used dilation and erosion operations to remove eyeglasses on the face. This produces better results than without this step.

An eye-state recognition technique based on eye pupil and iris detection can be applied for a DDS. Frame difference and geometrically deformed prototypes were used to detect eye pupils (Cyganek & Gruszczynski, 2013). Since the color of eyes is different from the color of a human face, color information was used for skin segmentation and to detect eyes in that region by Rajpathak *et al.* (2009). However, color information cannot be used in dark situations. Based on the properties of the eyes, circular object detection based on the Hough transform, was used to detect an eye pupil by See *et al.* (2014). In addition, edge detection was also applied by Azar and Khalilzadeh (2015) because eyes have complicated patterns and a high number of edge pixels. The location of eyes can then be estimated within the upper part of the human face. For iris recognition, pattern matching was used by the Euclidian distance technique (Adhau & Shedge, 2015) and the weighted majority voting technique (Ziauddin & Dailey, 2008).

All of the techniques mentioned above employ image intensities for their eye-state recognition steps. Consequently, they are all subject to lighting conditions. It is possible to apply image enhancement to make the recognition step be more robust to lighting conditions; however, image enhancement, requiring an extra computational cost, may not be consistently successful. Therefore, the objective of the proposed method is to use features that are more robust to various lighting conditions, the gradient and displacement vectors

3. Methodology

The input image consists of a driver's face and the car indoor background (Figure 1). This region is too large to be a region of interest (ROI) for eye detection and recognition with time complexity and errors of localization. To solve this problem, the ROI needs to be reduced to continue with the recognition process. Therefore, the proposed method is divided into 2 main parts:, localization and recognition (Figure 2). The process starts with localization. It is used to reduce the ROI from the input image by finding the locations of the face, pair of eyes, and center of the eyes. Then, we crop the region around the center of the eye. Next, the cropped region is used for eye state recognition. Since we deal with eye state recognition in dim and dark situations, IR LEDs were used. IR LEDs were on for all situations to provide a clear face, especially in dim and dark situations.

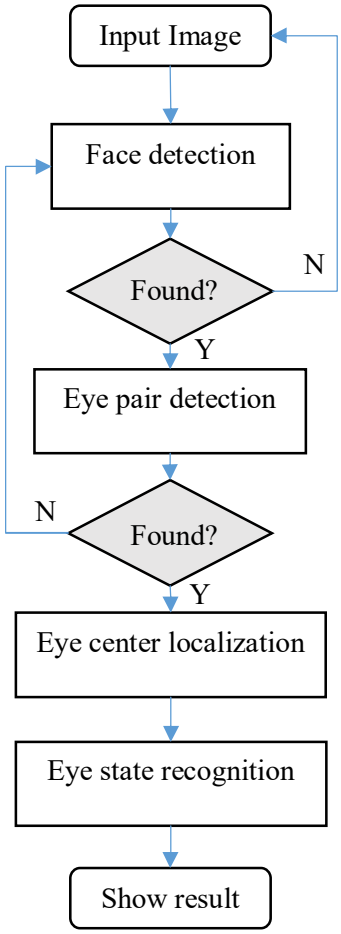

Figure 2. Flowchart of the proposed method.

3.1 Face and eye pair detection

This is the first step of the proposed method. The Haar cascade method proposed by Papageorgiou *et al.* (1998) was utilized in this research. It is used to detect and crop a face in the whole frame and a pair of eyes within the face region in the image. The Haar cascade method uses Haar like features and high and low intensity areas. The presence of Haar features is determined by subtracting the difference between high and low intensity areas. If the difference is less than a given threshold, the feature is said to be present. To guarantee that the correct object is recognized, the ROI must be trained with several Haar like features using about 100 patterns.

For face detection, we select the face that has the biggest area in the frame as a candidate to reduce false positives from passenger faces. However, only the up-right frontal face can be detected by this method. With different Haar like features, a pair of eyes is detected by the Haar cascade method if and only if a face exists. The red rectangular box in Figure 3a shows a face region detected, while the blue rectangular box shows a pair of eyes detected.

3.2 Eye center localization

A detected eye region is still a large region for recognition (Figure 3a). It can be reduced by cropping only the area around the center of the eye. We adopted the Fabain Timm method to localize the center of the eye (Timm & Barth, 2011), Circular object detection was obtained by finding the cosine angle between the gradient vector (g_i), obtained using the Sobel operators and displacement vectors on a candidate point ($d_{i,j}$) that can be calculated from Equations 1 and 2 on each point of interest (x_j) within the image. The displacement vectors were defined as radial vectors diverging from a pixel of interest in the eye region. It has been proven that normalized gradient vectors are not sensitive to lighting conditions (Kondo, 2014). In addition, displacement vectors are independent of intensity information. Therefore, this method is robust to various lighting conditions.

$$\mathbf{d}_{i,j} = x_i - x_j \tag{1}$$

$$\cos\theta_{i,j} = \frac{\mathbf{d}_{i,j} \cdot \mathbf{g}_i}{\left\|\mathbf{d}_{i,j}\right\|\left\|\mathbf{g}_i\right\|} \tag{2}$$

Figure 4a shows that a pixel of interest is located at the center of a dark circle. In this case, the displacement and gradient vectors have the same direction. It means that the cosine value between them is close to or equal to 1. By contrast, Figure 4b shows that a pixel of interest is located off the center of the circle. Then, the directions of the displacement and gradient vectors do not coincide with each other resulting in lower values of Equation 2. The score of each candidate point (S_j) is calculated by Equation 3 within the eye regions.

$$S_j = \frac{1}{N} \times \sum_{i}^{N} \cos\theta_{i,j} \tag{3}$$

where N is the number of pixels in the region of interest. The center of the eye is at the location with the maximum value, S_c. Figure 3b shows half of an eye pair region from the previous step. S_j at each candidate point is shown in Figure 3c. This shows that the highest score is produced at the center of the eye pupil. After we get the location of the center of the eye, we crop the region around the center of the eye for recognition in the next step. The cropped region is indicated by the green rectangular box in Figure 3d, and the cropped region is shown in Figure 3e.

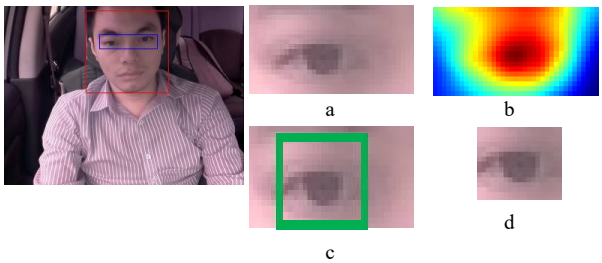

Figure 3. Localization results of (a) face and eye pair region, (b) a detected eye region, (c) S_c in the eye region, (d) marked area around eye centre, and (e) cropped area around eye center.

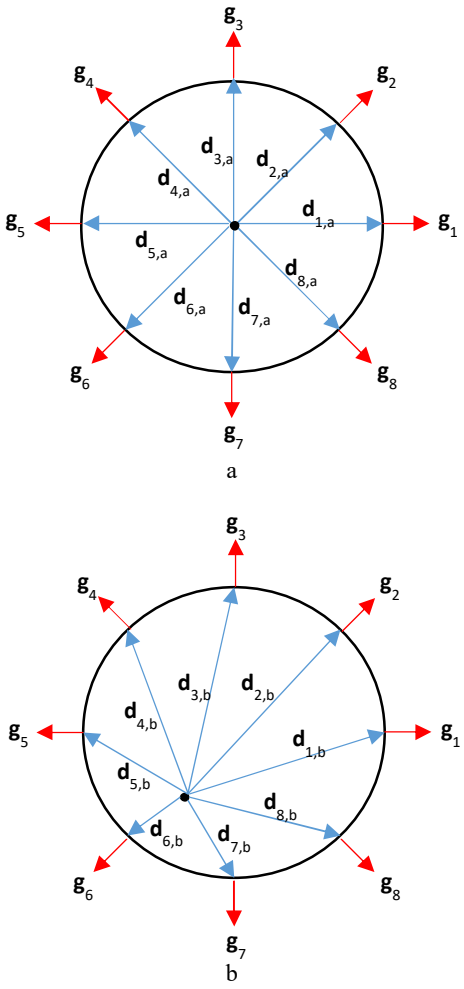

Figure 4. Displacement and gradient vectors when a pixel of interest lies (a) in the center of a circle and (b) off the center of a circle.

3.3 Eye state recognition

The eye region or cropped area from the previous step is used for recognition. In the experiment, we chose an eye region with high contrast for recognition. The left eye region is usually considered because the driver sits on the right side of cars in Thailand. Light illuminates the face on the right side more effectively. By thresholding the score, we use S_c of the eye region for classification because we assume that the center of the eye is located at this position based on the eye center localization step. For the open eye state, there is an eye pupil in the region (Figure 5a). For S_c of the open eye state in Figure 5b, it has a high value compared to the closed eye state score because of the unseen eye pupil of the closed eye state (Figure 5c, d). This shows that the area within the orange circle in Figure 5b and Figure 5d are effective for recognition.

After thresholding S_c, there is a chance for errors in recognition. To reduce the percentage of error, we used the previous and current eye state results in T_N milliseconds as the observed time. In Equation 4, t_c is the total time duration of the closed eye state by thresholding results. The number of frames that are recognized as a closed eye state is divided by the frame rate within period T_N. P is the percentage of the time period.

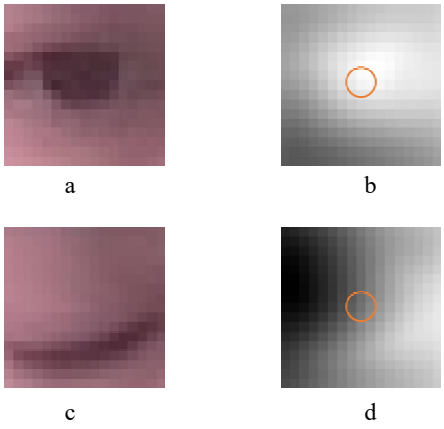

Figure 5. Eye regions of (a) open and (c) closed eye states and (b, d) their S_j matrix.

$$state = \begin{cases} close, t_c >= P \times T_N \\ open, otherwise \end{cases} \quad (4)$$

From Equation 4, we used the previous thresholding eye state result (ES_T), within T_N milliseconds to find the final results. If P and T_N are set to be 40% and 166.67 ms, respectively, or 2 of 5 frames for 30 fps, the final result is a closed eye state when two or more ES_T values are recognized as closed eye states. Otherwise, it is an open eye state as the final result.

4. Experimental Results

Our experiments were performed using C language with OpenCV 2.0 on a laptop PC with Intel core i5-3317U, 1.7 GHz, and 4GB of RAM. In the real experiment, a camera was located on the windshield at 45 cm from the driver's face (Figure 6a). A Pi NOIR camera, which is a regular camera module without an IR filter, was attached to a Raspberry Pi Type B Plus to record the sample videos at a frame rate of 30 fps (Figure 6b). The resolution of the input image was QQVGA (160×120). For IR LEDs, we used only an outer ring format to illuminate the face based on the experiment by Morimoto *et al.* (2000). IR LEDs are designed in the form of a bar to make them more suitable for a DDS (Figure 6b). The circuit consists of 8 IR LEDs, a resistor with 1000 ohms, and an 18 V voltage source connected in series. We captured 8 video sequences in bright, dim, and dark situations with and without illumination by IR LEDs. There were about 600 frames for each sample video. The brightness of each situation was measured by a Lux meter in the experiment. The average levels of brightness of bright, dim, and dark situations were 428.2, 25.0, and 0.5 LUX, respectively.

a b

Figure 6. Experimental setup of (a) driver position and (b) IR camera setting where IR LEDs, IR camera, and Raspberry Pi are shown in red, yellow, and blue rectangle boxes, respectively.

4.1 Accuracy of eye center localization

We evaluated the accuracies in locating the center of the eye. The correct locations were specified manually as the ground truth data. Table 1 shows the mean displacements between the detected locations and the ground truth data for the 8 video sequences (600 frames each) from 8 different persons. It showed that the mean displacements were 1 or 2 pixels only while the typical size of the pupil was about 7×7 pixels. As long as the displacement is within the eye pupil, we could proceed to the eye-state recognition step. Thus, the results were consistent and sufficiently accurate.

Table 1. Eye center localization accuracy.

Video sequence	Mean displacement (pixels)	SD
1	1.91	0.53
2	1.16	0.47
3	1.17	0.42
4	1.15	0.44
Mean	1.35	0.45

4.2 Recognition performance

In the recognition part, we set the parameters P and T_N in Equation 4 to be 0.4 (40%) and 166.67 ms, respectively. These values were determined through our experiments, empirically. To evaluate the recognition performance, a confusion table was constructed where closed eyes and open eyes states were considered as positive and negative results, respectively. We varied the threshold for the state recognition and used Equations 5 to 8 for evaluation.

$$\text{Recall} = \frac{TP}{TP + FN} \tag{5}$$

$$\text{Precision} = \frac{TP}{TP + FP} \tag{6}$$

$$\text{Specificity} = \frac{TN}{TN + FP} \tag{7}$$

$$\text{F1 score} = 2 \times \frac{\text{Recall} \times \text{Precision}}{\text{Recall} + \text{Precision}} \tag{8}$$

Figure 7 shows receiver operating characteristic (ROC) curves in bright, dim, and dark situations with various thresholds. In the dark situation, it shows only the result illuminated by IR LEDs (Figure 1c). For comparison, the areas under the curve are used: the larger the area, the better the performance. Based on the area under the curve, the best performance was achieved in the bright situation, while the second best came from the dark situation with the aid of IR LED illumination (Figure 7). The dim situation was the most difficult case because the visibility of the input image was worse than the other situations. IR LEDs increased the recognition performance in the dim situation effectively because the visibility of the eye pupils increased (Figure 1b). However, IR LEDs were less effective in bright situations.

From the experiment, we chose 0.4 as the threshold because it has the nearest result to the upper left corner in the ROC curve with 100% of recall and precision (Figure 7). For the input data, grayscale images were used for the traditional methods (Figures 8a-c) and S_j matrices were used for the proposed method in bright, dim, and dark situations (Figures 8d-f). They showed that the intensity of S_j matrices were almost the same in various situations while the grayscale image intensity was different.

Table 2 shows recognition in each situation from intensity projection (Zhang & Zhang, 2006), template matching (Veeraraghavan & Papanikolopoulos, 2001), and the proposed method. This demonstrated that both template matching and the proposed method were independent of lighting conditions because the F1 scores of each situation were quite similar to each other. With the aid of the IR LEDs, the average F1 score of the three techniques increased, especially in dim situations. In the overall situations, the proposed method had higher F1 scores on average than the other two methods.

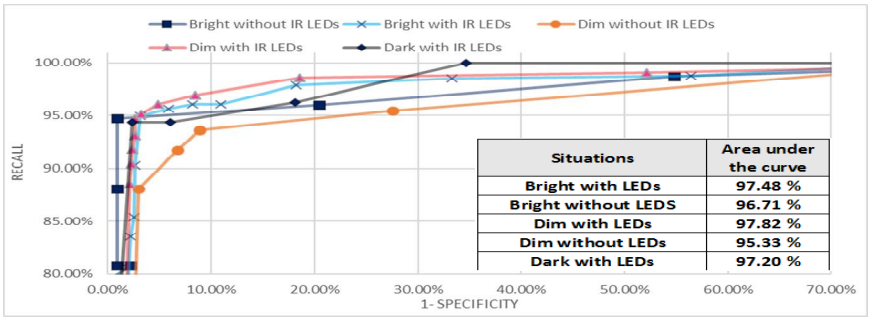

Figure 7. ROC curves in bright, dim, and dark situations with and without IR LEDs.

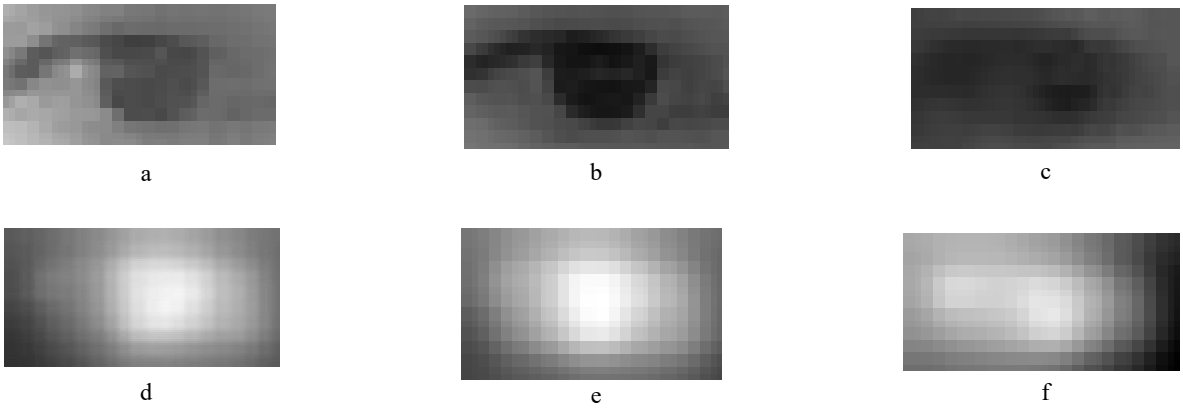

Figure 8. Grayscale image of eye regions in (a) bright, (b) dim, and (c) dark situations, and S_j matrix of eye regions in (d) bright, (e) dim, and (d) dark situations.

Table 2. Recognition performance.

Method	Measure	Without IR LEDs			With IR LEDs			
		Bright	Dim	Mean	Bright	Dim	Dark	Mean
Template matching	Recall	90.47%	78.06%	84.27%	89.85%	88.30%	80.71%	86.29%
	Precision	83.16%	87.81%	85.48%	88.95%	82.30%	87.78%	86.34%
	F1-score	86.18%	82.07%	84.13%	89.23%	84.80%	83.91%	85.98%
Intensity projection	Recall	88.72%	67.56%	78.14%	89.12%	84.14%	67.88%	80.38%
	Precision	89.09%	88.19%	88.64%	86.46%	87.81%	85.80%	86.69%
	F1-score	88.79%	75.23%	82.01%	87.37%	85.85%	75.15%	82.79%
Proposed method	Recall	91.20%	85.06%	88.13%	92.91%	90.72%	86.49%	90.04%
	Precision	90.83%	92.65%	91.74%	90.60%	91.30%	93.54%	91.81%
	F1-score	90.97%	88.35%	89.66%	91.69%	90.97%	89.76%	90.81%

4.3 Computation time

We measured the computation time of each process in the proposed method. The time consumptions in each step were 9.32 ms, 14.23 ms, and 0.09 ms for face and eye pair detection, eye center localization, and eye state recognition, respectively. Therefore, the total time of the proposed method was 23.64 ms. Time was used mainly in the eye center localization because of the calculation of displacement vectors. Since video clips had a frame rate of 30 fps or 33.3 ms per frame, the algorithm was complete within the time per frame. Therefore, the developed algorithm can be used in real time applications.

5. Conclusions and Future Work

We have proposed a driver drowsiness detection method using normalized cross-correlation between displacement vectors and gradient vectors. Since the displacement and gradient vectors were normalized in the computation of cross-correlation, the method worked well regardless of the varying intensities of an input image due to various lighting conditions. Initially the human face and eye region were detected in the image based on the Haar features. Within the eye region, we located a dark circular object that corresponded to the pupil. We tested the proposed method in three situations, bright, dim, and dark. Since IR LEDs consume little power, they were on to illuminate the face in all situations. The experimental results showed that the proposed method had a high performance in various lighting conditions. The computation cost of the proposed method was low and it works at video rates. In future works, we plan to improve the proposed method so it can be effective with a driver who wears glasses.

Acknowledgements

This research was financially supported by the Thailand Advanced Institute of Science and Technology (TAIST), National Science and Technology Development Agency (NSTDA), Japan Advanced Institute of Technology (JAIST), Tokyo Institute of Technology, National Research University Project, Thailand Office of the Higher Education Commission, and the Biomedical Engineering Research Unit, Sirindhorn International Institute of Technology (SIIT), Thammasat University (TU).

References

Adhau, A. S., & Shedge, D. K. (2015). Iris recognition methods of a blinked eye in nonideal condition. *International Conference on Information Processing 2015,* Pune, India. 75-79.

Akin, M., Kurt, M., Sezgin, N., & Bayram, M. (2008). Estimating vigilance level by using EEG and EMG signals. *Neural Computing and Applications, 17*(3), 227-236.

Anderson C., Chang, A. M., Sullivan, J. P., Ronda, J. M., & Czaisler C. A. (2013). Assessment of drowsiness based on ocular parameters detected by infrared reflectance oculography. *Journal of Clinical Sleep Medicine, 9*(9), 907 – 920.

Azar, A. R., & Khalilzadeh, F. (2015). Real time eye detection using edge detection and euclidean distance. *Proceedings of the International Conference on Knowledge-Based Engineering and Innovation 2005*, Tehran, Iran, 43-48.

Chang, C. W., Chou, L. H., Ho, M., & Chuan, C. C. (2013). A fatigue detection system with eyeglasses removal. *Proceedings of 15th International Conference on Advanced Communication Technology 2013*, Pyeongchang, South Korea, 331-335.

Cyganek, B., & Gruszczynski, S. (2013). Eye recognition in near-infrared images for driver's drowsiness monitoring. *Proceedings of IEEE Intelligent Vehi-cles Symposium 2013*, Gold Coast, Australia, 397-402.

Fazli, S., & Esfehani, P. (2012). Tracking eye state for fatigue detection. *Proceedings of International Conference on Advances in Computer and Electrical Engineering 2012*, Maharashtra, India, 17-20.

Garcia, I., Bronte, S., Bergasa, L. M., Almazan, J., & Yebes, J. (2012). vision-based drowsiness detector for real driving conditions. *Proceedings of Intelligent Vehicles Symposium 2012*, Alcalá de Henares, Spain, 618-623.

Healey, J. A., & Picard, R. R. (2005). Detecting stress during real-world driving tasks using physiological sensors. *Proceedings of Intelligent Transportation Systems, IEEE Transactions, 6*(2), 156-166.

Ingre, M., Akerstedt, T., Peters, B., Anund, A., & Kecklund, G. (2006). Subjective sleepiness, simulated driving performance and blink duration: Examining individual differences. *Journal of Sleep Research, 15* (1), 47-53.

Kawakita, E., Itoh, M., & Oguri, K. (2010). Estimation of driver's mental workload using visual information and heart rate variability. *Proceedings of 13th International IEEE Conference on Intelligent Transportation Systems*, Madeira Island, Portugal, 765-769.

Kokonozi, A. K., Michail, E. M., Chouvarda, I. C., & Maglaveras, N. M. (2008). A study of heart rate and brain system complexity and their interaction in sleep- deprived subjects. *Proceedings of Computer in Cardiology 2008*, Bologna, Italy, 969-971.

Kondo, T. (2014). Gradient orientation pattern matching with the Hamming distance. *Pattern Recognition, 47*(10), 3387-3404.

Liu, C. C., Hosking, S. G., & Lenne, M. G. (2009). Predicting driver drowsiness using vehicle measures: Recent insights and future challenges. *Journal of Safety Research, 40*(4), 239-245.

Morimoto, C., Koons, D., Amir, A., & Flickner, M. F. (2000). Pupil detection and tracking using multiple light sources. *Image and Vision Computing, 18*(4), 331-335.

Papageorgiou, C. P., Oren, M., & Poggio, T. (1998). A general framework for object detection. *Proceedings of International Conference on Computer Vision 1998*, Bombay, India, 555-562.

Rajpathak, T., Kumar, R., & Schwartz, E. (2009). Eye detection using morphological and color image processing. *Proceedings of Florida Conference on Recent Advances in Robotics 2009*. Florida, FL, 1-6.

Salvucci, D. D., & Liu, A. (2002). The time course of lane change: Driver control and eye movement behavior. *Transportation Research Part F: Traffic Psychology and Behavior, 5*(2), 123-132.

See, Y. C., Noor, N. M., & Rijal, O. M. (2014). Hybrid method of iris detection based on face localization. *TENCON 2014*, Bangkok, Thailand, 1-5.

Sigari, M. H., Fathy, M., & Sorayani, M. (2013). Driver face monitoring system for fatigue and distraction detection. *International Journal of Vehicular Technology*. 1-11.

Sooksatra, S., Kondo, T., & Bunnun, P. (2015). A robust method for drowsiness detection using distance and gradient vectors. *Proceedings of International Conference on Electrical Engineering/Electronics Computer, Telecommunications and Information Technology 2015*, Hua Hin, Thailand, 1-5.

Timm, F., & Barth, E. (2011). Accurate eye centre Localization by means of gradients. *Proceedings of the International Conference on Computer Theory and Applications 2011*, Algarve, Portugal, 125-130.

Veeraraghavan, H., & Papanikolopoulos, N. P. (2001). *Detecting driver fatigue through the use of advanced face monitoring techniques*. Washington, DC: Intelligent Transportation System Institute.

Wilkinson, V. E., Jackson, M. L., Westlake J., Stevens B., Barnes, M., Swann, P., . . . Howard, M.E. (20130. The accuracy of eyelid movement parameters for drowsiness detection. *Journal of Clinical Sleep Medicine, 9*(12), 1315 – 1324.

Yutian, F., Dexuan, H., & Pingqiang, N. (2009). A combined eye states identification method for detection of driver fatigue. *Proceedings of Wireless Mobile and Computing 2009*, Marrakech, Morocco, 217-220.

Zhang, Z., & Zhang, J. (2006). A new real-time eye tracking for driver fatigue detection. *Proceedings of 6th International Conference on ITS Telecommunications Proceedings 2006*, Chengdu, China, 8-11.

Ziauddin, S., & Dailey, M. N. (2008). Iris recognition performance enhancement using weighted majority voting. *IEEE International Conference on Image Processing 2008*, San Diego, CA, 277-280.